In situ hybridization of PNA/DNA studied label-free by electrochemical impedance spectroscopy†

Jianyun Liu,[a] Shengjun Tian,[a] Peter E. Nielsen[b] and Wolfgang Knoll*[a]

Received (in Cambridge, UK) 5th January 2005, Accepted 13th April 2005
First published as an Advance Article on the web 29th April 2005
DOI: 10.1039/b419425j

The *in situ* hybridization kinetics of label-free DNA on mixed monolayers of peptide nucleic acid (PNA) and 6-mercapto-1-hexanol (MCH) on Au electrodes was investigated by electrochemical impedance spectroscopy (EIS) and used to discriminate the fully complementary DNA from the single-base mismatched hybrids.

The detection of DNA hybridization is of significant scientific and technological importance, as manifested, for example, in the growing interest in chip-based characterization of gene expression pattern and detection of pathogens. The details of such surface confined DNA hybridization reactions are important for the *in situ* control of binding events and for selecting the optimal reaction conditions. A number of groups have described successful attempts to monitor surface hybridization reaction kinetics by optical detection, such as scanning fluorescence in an array format,[1] surface plasmon resonance spectroscopy,[2,3] or surface plasmon fluorescence spectroscopy.[4] Electrochemical concepts have also proven to be very useful for sequence-specific biosensing of DNA, because they provide simple, rapid, label-free and low-cost detection of nucleic acid sequences.[5,6] Among the used electrochemical techniques, electrochemical impedance spectroscopy (EIS) has been shown to be very effective and sensitive for the characterization of biomaterial-functionalized electrodes and biocatalytic transformations at electrode surfaces. It allows for the analysis of interfacial changes originating from biorecognition events at electrode surfaces.[7] Li *et al.* had used EIS to investigate the electron transfer in the DNA duplexes film,[8] and the single mismatch by binding MutS protein to the DNA duplex.[9] Willner's group used EIS to detect the DNA/DNA interaction by means of an enzyme-linked amplification or a biotin–avidin architecture for amplification.[10–13] On the polypyrrole–DNA film, the detection of the hybridization event by EIS was also demonstrated recently based on the electrochemical activity of pyrrole.[14] However, the data obtained above were all based on the comparison of the different electrochemical signals before and after hybridization. Until now, there is no report yet about the *in situ* reaction kinetics of DNA hybridization monitored by electrochemical methods. However, this information is crucial to studies on biosensors[15] and DNA-driven assembly strategies.[16]

In this communication, we present *in situ* hybridization kinetic studies with label-free DNA target oligonucleotides on a mixed monolayer of PNA and MCH on Au electrodes using EIS. The principle of impedimetric sensing of DNA hybridization is based on the formation of nucleic acid/DNA complexes at an electrode surface. The resulting negatively charged interface electrostatically repels the negatively charged redox indicator $Fe(CN)_6^{3-/4-}$. The electrostatic repulsion of the redox-active molecules leads to an enhanced charge transfer resistance, R_{ct}. Thus, R_{ct} will increase with the increasing amount of hybridized DNA. Hence, EIS can be used to follow the *in-situ* hybridization kinetics of PNA/DNA by recording the change of R_{ct} with time.

PNA is a DNA mimic that has a neutral peptide-like backbone with nucleobases that allows for the molecules to hybridize to complementary DNA strands with high affinity and specificity.[17] The immobilized PNA probes on the sensor surface are uncharged, and hence, do not affect the charge transfer from the redox indicator $Fe(CN)_6^{3-/4-}$ to the electrode. Once DNA targets hybridize to PNA, the charge density at the sensor surface will be changed. Thus, one can use EIS to conveniently monitor the PNA/DNA hybridization process.

Table 1 shows the thiol-terminated PNA probe and DNA target sequences used in this study. Thiolated PNAs were assembled on the gold electrode surface by gold–thiol bonds. The desired probe density on the surface was obtained by controlling the exposure time and concentration of the probe solution. Here, PNA-modified surfaces were obtained by exposing the gold substrates in a 200 nM PNA solution for about 10 h. The surfaces were then treated further with 1 mM mercaptohexanol (MCH) solution for 1 h. An EC flow cell was used with an inlet and outlet for solution circulation. Fig. 1 shows the faradaic impedance spectra of the PNA-modified surface in 20 mM phosphate buffer solution in the presence of fully complementary DNA targets (c_0 = 500 nM) and the $Fe(CN)_6^{3-/4-}$ redox indicator after different hybridization times. Clearly, R_{ct} (the diameter of the semicircle of the Nyquist plot) increases gradually with increasing hybridization time. This is consistent with the electrostatic repulsion of the redox indicator from the electrode interface by the formation of the charged PNA/DNA duplexes, thereby introducing a barrier for interfacial

Table 1 The sequences of PNA probe and DNA targets

Name	Sequence
Thiolated PNA[a]	Cys-[eg1]$_6$TGT ACA TCA CAA CTA-NH_2
Fully complementary target	5′-TAG TTG TGA TGT ACA
Target with one mismatch	5′-TAG TTG TGA *C*GT ACA
Target with two mismatch	5′-TAG TTG TCA *C*GT ACA
Completely mismatched target	5′-*ATC AAC ACT ACA TGT*

[a] Cys(egl)$_6$: 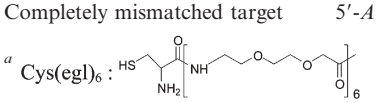

† Electronic supplementary information (ESI) available: SPFS results and the kinetics on regeneration substrates. See http://www.rsc.org/suppdata/cc/b4/b419425j/

*knoll@mpip-mainz.mpg.de

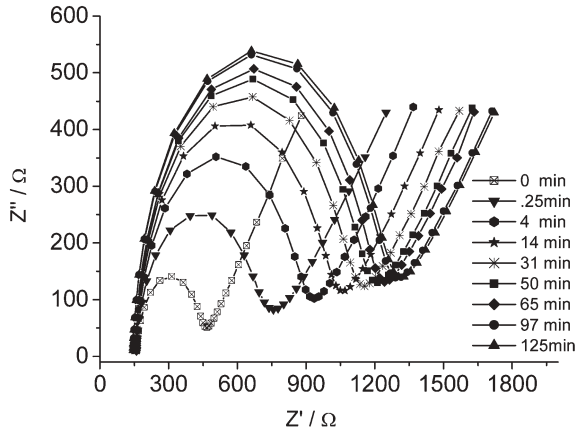

Fig. 1 Nyquist plots of PNA/DNA hybridization in 20 mM PBS containing 500 nM fully complementary target and 1 mM/1 mM $Fe(CN)_6^{3-/4-}$ with different hybridization time. The imaginary impedance (Z'') and the real impedance (Z') are recorded as a function of the applied frequency.

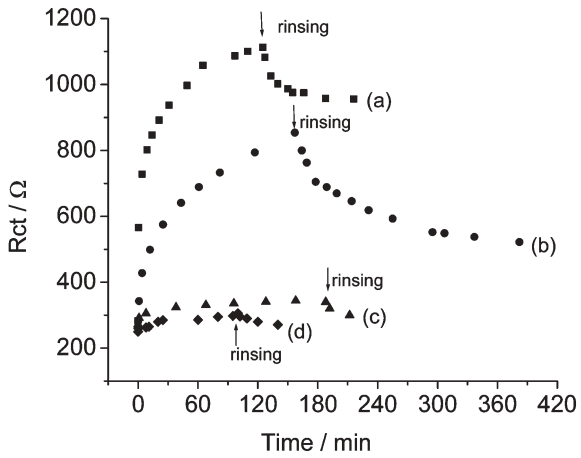

Fig. 2 PNA/DNA hybridization kinetics. R_{ct} is obtained from the fitting of impedance spectrum. (a) fully complementary DNA target, (b) one base mismatch, (c) two bases mismatch and (d) complete mismatch, respectively.

electron transfer. After ~2 hours, R_{ct} reached a plateau value, indicating that the hybridization reaction reached its equilibrium. Upon rinsing the surface with PB solution containing only the $Fe(CN)_6^{3-/4-}$ redox indicator, R_{ct} decreased with longer rinsing times due to the dissociation of the DNA/PNA duplex on the surface. By plotting the Rct values[18] versus the corresponding reaction time (Fig. 2 curve a), the association and dissociation kinetics of the fully matched DNA/PNA duplex can be obtained.

Curve b in Fig. 2 gives the association and dissociation kinetics found for a single-base mismatched target. The difference between the association processes of the fully matched and the single-base mismatched targets is not so significant and is similar to that of the fluorescence detection reported elsewhere.[4] However, for the dissociation process, R_{ct} value was still decreasing even though the surface was rinsed for a longer time (it takes more than 10 h to finish the full desorption of the single-base mismatched targets[4]). While the dissociation of fully matched targets can reach equilibrium within 1 h. The difference of the binding behaviors can be seen even more clearly by comparing the exact binding constants (*vide post*, *cf.* table 2). This method, hence, can discriminate a single-base mismatch directly. Moreover, the addition of a two-base mismatched target or of a completely mismatched DNA target under identical conditions, did not show any clear R_{ct} change (curve c and d of Fig. 2), which indicates that nonspecific adsorption of DNA targets to the PNA-modified surface is insignificant.

Further information about the DNA/PNA hybridization process can be obtained from titration experiments. Fig. 3 (A) presents the results of the corresponding experiment with increasing concentration of the fully complementary target. A 1 nM target solution leads to a clearly detectable binding of complementary sequences. After injection of target DNA solutions with increasing concentration, R_{ct} increases as a function of time. Assuming that a Langmuir model is suitable for the treatment of interfacial PNA/DNA reactions,[19,20] theoretical fit curves were calculated (given in Fig. 3 (A), solid lines), and found to be in good agreement with the experimental curves. The corresponding association rate constant k_{on}, the dissociation rate constant k_{off} and the affinity constant K_A (given by $K_a = k_{on}/k_{off}$) are shown in Table 2.

Another way to analyse the K_a value is based on the Langmuir adsorption isotherm. According to $R_{ct} = (R_{ct})_{max}\, c_0 K_A/(1 + c_0\, K_A)$, a plot of c_0/R_{ct} as a function of c_0 yields a straight line from which the affinity constant K_A can be deduced. This plot together with a linear regression is shown in Fig. 3 (B), resulting in $K_A = 6.6 \times 10^7\ M^{-1}$. Similarly, for single-base mismatch, K_A is around $8.0 \times 10^6\ M^{-1}$, which is in agreement with the results reported elsewhere.[21]

In order to check the reliability of the EIS method for *in situ* monitoring DNA hybridization, we also carried out repeated experiments on different samples or regeneration experiment on the same substrate under the same conditions (ESI†, Fig. S1). All the results are reproducible and show very similar hybridization kinetics.

For comparison, surface plasmon resonance enhanced fluorescence spectroscopy (SPFS) was used to detect the affinity constants on the same architecture. The detailed experimental setup was the same as described in the literature.[4,20] The DNA target used for the

Table 2 Kinetic data, *i.e.* the association (k_{on}) and dissociation rate constant (k_{off}) and affinity rate constant K_A

Target	$k_{on}/M^{-1}\ min^{-1}$	k_{off}/min^{-1}	$K_A{}^a/M^{-1}$	$K_A{}'^b/M^{-1}$	$K_A{}''^c/M^{-1}$
Fully complementary DNA	6.2×10^4	1.7×10^{-3}	3.6×10^7	6.6×10^7	8.9×10^7
Single-base mismatch DNA	2.4×10^4	$4.1 \times 10-3$	5.7×10^6	8.0×10^6	1.5×10^7

[a] K_a is the fit based on the Langmuir model for the adsorption and desorption behavior with the time-dependent equation. [b] K_a' is the fit from the relationship between R_{ct} and concentration based on the Langmuir adsorption isotherm. [c] K_a'' was obtained from SPFS using Cy5-labeled DNA as target.

 This journal is © The Royal Society of Chemistry 2005

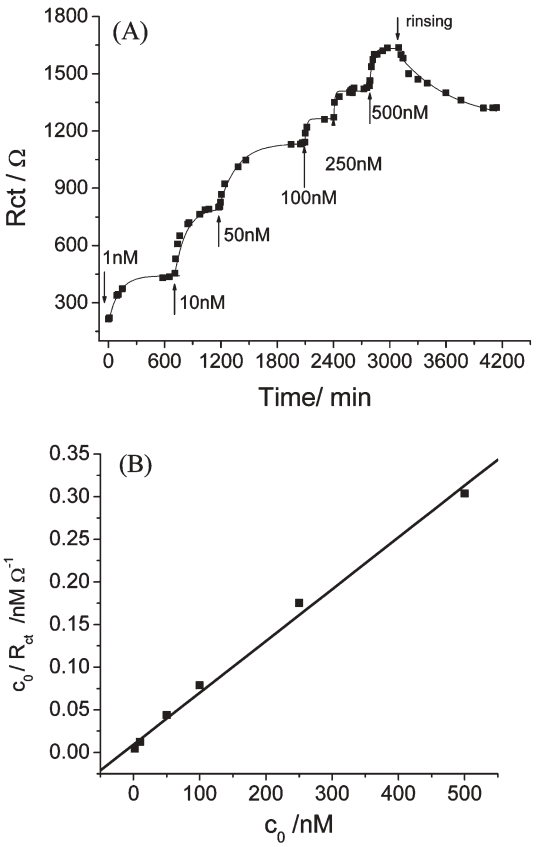

Fig. 3 (A) hybridization kinetics of PNA/DNA on thiolated PNA modified Au surface with increasing complementary target concentration in the flow cell. (B) Linearized plot of Langmuir isotherm of the data presented in Fig. 3 (A).

SPFS detection has the same base sequence as that employed in EIS, but with a cyanine dye (Cy5) as a label at the 5′ end. The fluorescence was monitored as a function of time for each concentration. After equilibration was reached, the sample was shortly rinsed, and an angular SPFS scan was taken (ESI†, Fig. S2). The affinity constants obtained for the complementary and the single-base mismatched DNA hybridization reactions are collected in Table 2, together with the results from the impedance measurements. One can see that the results from the SPFS give slightly higher affinity constants than those derived from EIS. However, the difference is within the experimental accuracy.

In conclusion, we demonstrated for the first time that EIS is a simple and convenient technique for the *in situ* kinetic analysis of DNA hybridization. A single-base mismatch can be directly seen in the kinetic curves. Moreover, the exact association (hybridization) and dissociation rate constants can be obtained. Thus, the method is comparable to a fluorescence technique. Detailed experiments on ionic strength, probe density and temperature effects, as well as, a comparison with DNA/DNA hybridization are under way.

This work was partly supported by the Deutsche Forschunggemeinschaft (DFG, KN 224/13-1).

Jianyun Liu,[a] Shengjun Tian,[a] Peter E. Nielsen[b] and Wolfgang Knoll*[a]
[a]*Max-Planck-Institute for Polymer Research, Ackermannweg 10, D-55128, Mainz, Germany. E-mail: knoll@mpip-mainz.mpg.de; Fax: +49-6131-379360; Tel: +49-6131-379160*
[b]*Center for Biomolecular Recognition, Department for Biochemistry and Genetics, Biochemistry Laboratory B, The Panum Institute, Blegdamsvej 3c, DK-2200, Copenhagen, Denmark*

Notes and references

1 P. A. E. Piunno, U. J. Krull, R. H. E. Hudson, M. J. Damha and H. Cohen, *Anal. Chim. Acta*, 1994, **288**, 205.
2 D. Piscevic, R. Lawall, M. Veith, Y. Okahata and W. Knoll, *Appl. Surf. Sci.*, 1995, **90**, 425.
3 R. Georgiadis, K. P. Peterlinz and A. W. Peterson, *J. Am. Chem. Soc.*, 2000, **122**, 3166.
4 T. Liebermann, W. Knoll, P. Sluka and R. Herrmann, *Colloid Surf., A*, 2000, **169**, 337.
5 J. Wang, *Nucleic Acids Res.*, 2000, **28**, 3011.
6 F. Patolsky, E. Katz, A. Bardea and I. Willner, *Langmuir*, 1999, **15**, 3703.
7 E. Katz and I. Willner, *Electroanalysis*, 2003, **15**, 913.
8 Y. Long, C. Li, H. Kraatz and J. S. Lee, *Biophys. J.*, 2003, **84**, 3218.
9 C. Li, Y. Long, J. S. Lee and H. Kraatz, *Chem. Commun.*, 2004, 574.
10 L. Alfonta, A. Bardea, O. Khersonsky, E. Katz and I. Willner, *Biosens. Bioelectron.*, 2001, **16**, 675.
11 F. Patolsky, A. Lichtenstein and I. Willner, *Chem.-Eur. J.*, 2003, **9**, 1137.
12 F. Patolsky, A. Lichtenstein and I. Willner, *J. Am. Chem. Soc.*, 2001, **123**, 5194.
13 L. Alfonta, A. K. Singh and I. Willner, *Anal. Chem.*, 2001, **73**, 91.
14 C. M. Li, C. Q. Sun, S. Song, V. E. Choong, G. Maracas and X. J. Zhang, *Front. Biosci.*, 2005, **10**, 180.
15 K. U. Mir and E. M. Southern, *Nat. Biotechnol.*, 1999, **17**, 788.
16 J. J. Storhoff and C. A. Mirkin, *Chem. Rev.*, 1999, **99**, 1849.
17 P. E. Nielsen, M. Egholm, R. H. Berg and O. Buchardt, *Science*, 1991, **254**, 1497.
18 R_{ct} value was obtained by fitting the Nyquist plot using the normal Randles equivalent circuit (see ref. 12).
19 T. Neumann, M. L. Johansson, D. Kambhampati and W. Knoll, *Adv. Funct. Mater.*, 2002, **12**, 575.
20 D. Kambhampati, P. E. Nielsen and W. Knoll, *Biosens. Bioelectron.*, 2001, **16**, 1109.
21 K. K. Jensen, H. Ørum, P. E. Nielsen and B. Norden, *Biochemistry*, 1997, **36**, 5072.